Crystallization in Hybrid Organic−Inorganic Materials Induced by Self-Organization in Basic Conditions

Bouzid Menaa,[†,‡] Masahide Takahashi,[†,‡] Plinio Innocenzi,*[,§] and Toshinobu Yoko[†]

Institute for Chemical Research, Kyoto University, Gokasho, Uji, Kyoto 611-0011, Japan, PRESTO, Japan Science and Technology Agency, Kawaguchi, Saitama 332-0012, Japan, and Dipartimento di Architettura e Pianificazione, Laboratorio di Scienza dei Materiali e Nanotecnologie, INSTM and Nanoworld Institute, Università di Sassari, Palazzo Pou Salit, Piazza Duomo 6, 07041 Alghero (Sassari), Italy

Received November 8, 2006. Revised Manuscript Received December 31, 2006

Hybrid organic−inorganic crystalline materials have been obtained from a simple solvent-free synthesis in highly basic conditions. The formation of an organized hybrid structure has been achieved for the first time via sol−gel without employing bridged organosilica precursors. 3-glycidoxypropyltrimethoxysilane, which is an organically modified alkoxide bearing a terminal epoxy group, has been used for the synthesis. The opening of the epoxy has been observed to produce poly/oligo(ethylene oxide) chains or *p*-dioxane species. In the second case crystalline hybrids have been formed by self-organization during gelation. Analysis performed by wide-angle X-ray scattering and X-ray diffraction have confirmed the crystalline nature of the aggregates, epoxy ring opening/self-condensation which resulted in a pillared-type organic−inorganic hybrid structure with Si-substituted 2,5-bis(propoxymethyl)-1,4-dioxane organic spacer as pillar.

Introduction

Organic−inorganic hybrids[1] are a fascinating class of materials whose structure typically shows a disordered state. Sol−gel processing of these materials gives in most cases the formation of amorphous structures, and a glassy-disordered phase represents the most common texture in hybrids. The only exception to this rule of thumb is represented by bridged silsesquioxanes.[2] This group of hybrid materials forms a three-dimensional structure and can be distinguished from other silsesquioxanes because the organic groups are directly part of the interconnected organic−inorganic network.[3] The bridged silsesquioxanes are synthesized by sol−gel processing of precursors having different types of bridging organic species and two or more trifunctional silyl groups. These materials can be easily designed through the modification of the bridging organic group, and even if organization is a very difficult task to achieve in hybrids, they can exhibit, in the proper conditions, a surprising tendency to self-organize in "crystalline" structures. Long-range order through self-organization has been, in fact, observed using very specific organic precursors,[4] solid-state routes,[5] or bridged organosilane precursors.[6] The weak interactions between the organic units during hydrolysis and condensation of $(RO)_3Si-R'-Si(OR)_3$ precursors represent the key to auto-organization in bridged polysilsesquioxanes.[7] Several hybrid structures with different ranges of order, from nano- to microscale have been obtained. An intriguing example of the self-organization ability of bridged organosilane precursors has been shown by Inagaki et al. that used benzene bridged organosilane alkoxides to obtain ordered pore walls in mesoporous hybrid materials.[8]

Direct crystallization of hybrid materials by hydrolytic sol−gel reactions of nonbridged organically modified alkoxides represents, instead, a much more challenging task, and no examples have been reported up to now. In the present work we have been able, however, to achieve the formation of crystalline structures using an organically modified alkoxide bearing an epoxy functional group, 3-glycidoxypropyltrimethoxysilane (GPTMS), as precursor. GPTMS is an organofunctional alkoxysilane that is widely used as a result of the several important applications in photonics and electronic.[9] The organic part contains an epoxy ring that can be cross-linked to form a poly(ethylene oxide) chain and can behave, therefore, as a network former.[12] Sol−gel synthesis of GPTMS based hybrid materials is quite complex because

* To whom correspondence should be addressed. E-mail: plinio@uniss.it.
† Kyoto University.
‡ Japan Science and Technology Agency.
§ Università di Sassari.

(1) (a) Sanchez, C.; Lebeau, B.; Chaput, F.; Boilot, J.-P. *Adv. Mater.* **2003**, *15*, 1969. (b) Davis, M. E. *Nature* **2002**, *417*, 813.
(2) Corriu, J. P. *Angew. Chem., Int. Ed.* **2000**, *39*, 1376.
(3) Shea, K. J.; Loy, D. A. *Chem. Mater.* **2001**, *13*, 3306.
(4) (a) Moreau, J. J. E.; Vellutini, L.; Man, M. W. C.; Bied, C.; Bantignies, J.-L.; Dieudonné, P.; Sauvajol J. L. *J. Am. Chem. Soc.* **2001**, *123*, 7957. (b) Moreau, J. J. E.; Vellutini, L.; Man, M. W. C.; Bied, C. *J. Am. Chem. Soc.* **2001**, *123*, 1509.
(5) Muramatsu, H.; Corriu, R. J. P.; Boury, B. *J. Am. Chem. Soc.* **2003**, *125*, 854.
(6) (a) Cerveau, G.; Corriu, R. J. P.; Framery, E.; Lerouge, F. *Chem. Mater.* **2004**, *16*, 3794. (b) Ben, F.; Boury, B.; Corriu, R. J. P.; Le Strat, V. *Chem. Mater.* **2000**, *12*, 3249. (c) Boury, B.; Corriu, R. J. P.; Delord, P.; Le Strat, V. *J. Non-Cryst. Solids* **2000**, *265*, 41.
(7) Ben, F.; Boury, B.; Corriu, R. J. P. *Adv. Mater.* **2002**, *14*, 1081.
(8) Inagaki, S.; Guan, S.; Ohsuna, T.; Terasaki, O. *Nature* **2002**, *416*, 304.
(9) Popall, M.; Kappel, J.; Pilz, M.; Schulz, J.; Feyder, G. *J. Sol-Gel Sci. Technol.* **1994**, *2*, 157. (b) Schmidt, H. *J. Non-Cryst. Solids* **1994**, *178*, 302. (c) Sorek, Y.; Reisfeld, R.; Tenne, R. *Chem. Phys. Lett.* **1994**, *227*, 235. (d) Innocenzi, P.; Brusatin, G.; Guglielmi, M.; Signorini, R.; Bozio, R.; Maggini, M. *J. Non-Crystal. Solids* **2000**, *265*, 68. (e) Signorini, R.; Meneghetti, M.; Bozio, R.; Maggini, M.; Scorrano, G.; Prato, M.; Brusatin, G.; Innocenzi, P.; Guglielmi, M. *Carbon* **2000**, *38*, 1653.
(10) Schottner, G. *Chem. Mater.* **2001**, *13*, 3422.

10.1021/cm062660u CCC: $37.00
Published on Web 03/14/2007

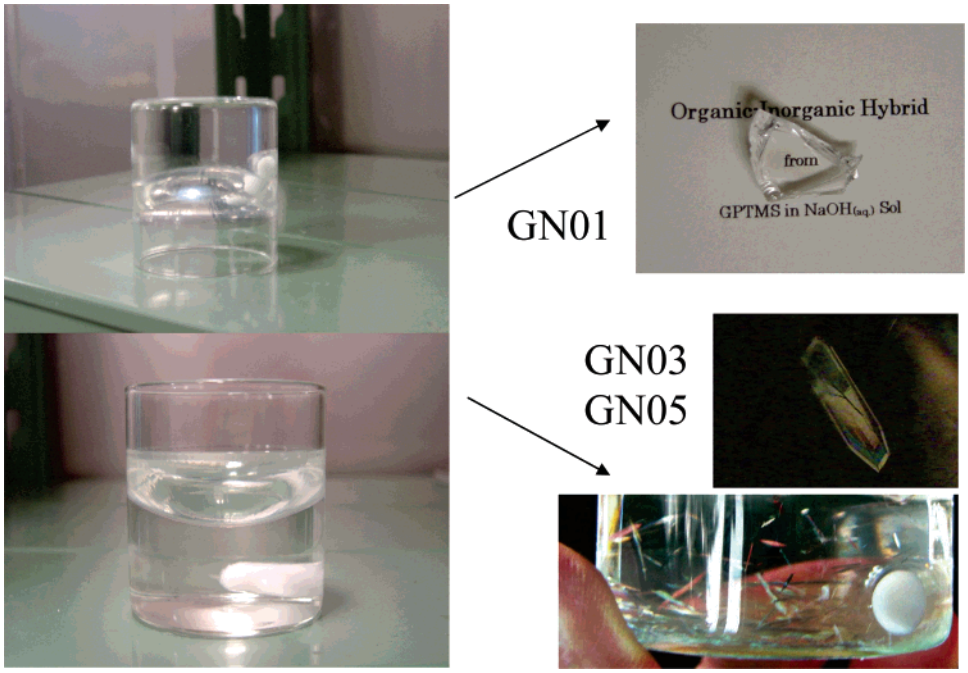

Figure 1. Photography of the hybrid crystals spread in the transparent gel. (right, in the middle) A polarized microscopy picture (× 20) of a single polygonal thin-plate crystal within the gel.

the opening of the epoxy can follow several possible reaction pathways. The epoxy can either undergo hydrolysis or alcoholysis to form the corresponding diol or β-hydroxy ethers or polyaddition reactions to form polyether chains.[10] A full control of the synthesis is, therefore, quite difficult to achieve, and different products from the epoxy opening can be observed in the final material. Furthermore the reactivity of GPTMS is not very high, and for sol−gel processing a long reaction time in presence of a catalyst is necessary.

The synthesis of hybrid materials based on GPTMS and more in general when organically modified alkoxides containing polymerizable organic functional groups are involved is realized through a delicate balance of the polycondensation of the inorganic network and the epoxy opening reactions.[11] An important role is played by the catalyst: the type (acid, base, Lewis acid, etc.) and relative amount strongly affect the structure of the final material.[12] It has been observed, in fact, that a faster inorganic polycondensation with respect to the reaction of the polymerizable organic groups hinders the formation of extended organic chains.[11b] The hybrid structure can be, therefore, tuned, within some limits, by controlling the kinetics of the organic and inorganic reactions of the organically modified alkoxides in the precursor sol. Because the epoxy groups in GPTMS have been shown to form different types of cross-linked organic structures in sol−gel acidic and basic[13] synthesis we have tried to use this ability to obtain in situ organic bridging groups that can favor self-organization into crystalline structures. A solvent free reaction should allow a better control of the final product, and we have therefore used only water and the basic catalyst for the sol−gel synthesis of GPTMS.

We have successfully obtained, via a basic synthesis of GPTMS, the formation of macroscopic long-range ordered crystals. This result has been achieved for the first time in hybrid materials without employing bridging alkoxides as precursors.

Experimental Section

Materials Synthesis. GPTMS (99%) was purchased from Shin-Etsu, Japan, and used without further purification. NaOH in solid pellets (97%, Waco Chemical Industries, Japan) and distilled water were employed as the catalyst and for hydrolysis, respectively. Using GPTMS as precursor, we synthesized three different sols, by a solvent-free reaction in highly basic conditions using the following molar ratios: $GPTMS/H_2O/NaOH = 1:5:x$, where $x =$ 0.1 (GN01), 0.3 (GN03), and 0.5 (GN05).

The sols were prepared by this procedure: NaOH was ground and poured into a 50 mL Pyrex beaker before adding distilled water (12 mL). After observing the complete dissolution of NaOH, GPTMS (30 mL) was then added under stirring. After the addition of GPTMS the sols became opaque, turned to transparent within a couple of minutes, and finally formed a transparent gel. The beakers with the sols were thereafter covered for 24 h with a Parafilm. After this time the sols were dried in air at room temperature (20 °C) with a relative humidity RH = 30% for 10 days. A transparent gel was obtained in the case of sample GN01, while GN03 and GN05 were characterized by the additional formation of crystals within the gel. In GN03 and GN05, thin plate-shaped formations, ∼1−2 mm long and ∼200−1000 μm thick, were observed. These macroscopic aggregates (Figure 1) were spread into the hybrid gels.

The powdered samples were washed with distilled water and dried at 60 °C; these samples were then analyzed by a series of

(11) (a) Innocenzi, P.; Brusatin, G.; Guglielmi, M.; Bertani, R. *Chem. Mater.* **1999**, *11*, 1672−1679. (b) Innocenzi, P.; Brusatin, G.; Babonneau, F. *Chem. Mater.* **2000**, *12*, 3726.

(12) (a) Hoebbel, D.; Nacken, M.; Schmidt, H. *J. Sol-Gel Sci. Technol.* **1998**, *12*, 169. (b) Popall, M.; Durand, H. *Electrochim. Acta* **1992**, *37*, 1593. (c) Riegel, B.; Blittersdorf, S.; Kiefer, W.; Hofacker, S.; Muller, M.; Schottner, G. *J. Non-Cryst. Solids* **1998**, *226*, 76. (d) Alonso, B.; Massiot, D.; Babonneau, F.; Brusatin, G.; Della Giustina, G.; Kidchob, T.; Innocenzi, P. *Chem. Mater.* **2005**, *17*, 3172.

(13) (a) Brusatin, G.; Innocenzi, P.; Guglielmi, M.; Babonneau, F. *J. Sol-Gel Sci. Technol.* **2003**, *26*, 303. (b) Innocenzi, P.; Kidchob, T.; Yoko, T. *J. Sol-Gel Sci. Technol.* **2005**, *35*, 225.

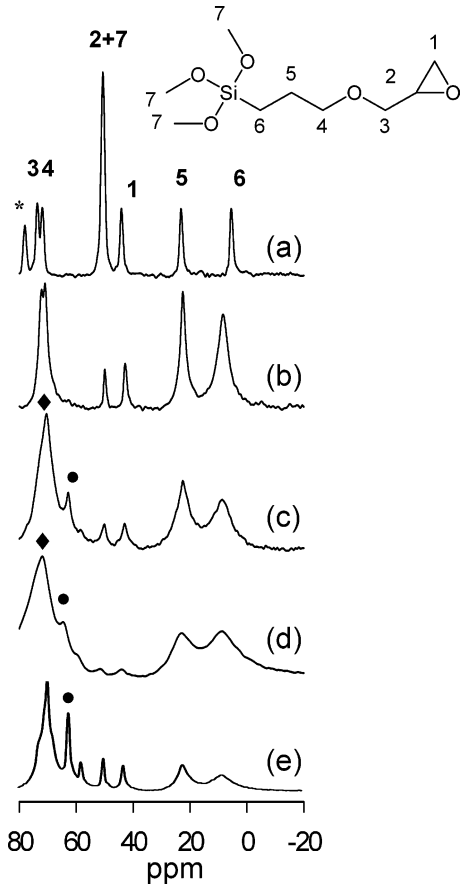

Figure 2. ^{13}C solution NMR spectrum for (a) GPTMS (* = $CDCl_3$ carbon at 78 ppm) and ^{13}C MAS NMR solid-state spectra for (b) GN01, (c) GN03, and (d) GN05 after 10 days of aging and (e) crystal part mechanically separated from sample shown in part d (signal at 74 ppm (symbol ◆) is attributed to the carbons in the poly(ethylene oxide) chains (−O−CH_2−[CH_2−$CH2$−]$_n$−O−)). For the spectra c and d, the signal annotated with a black circle (symbol ●) corresponds to the methylene carbon (CH_2) of the dioxane ring at 68 ppm. The inset corresponds to the GPTMS molecule with the different carbon atoms marked from 1 to 7 for NMR signals assignment.

techniques including X-ray diffraction (XRD), wide-angle X-ray scattering (WAXS), ^{13}C and ^{29}Si solid-state magic angle spinning (MAS) nuclear magnetic resonance (NMR) and solution NMR, Fourier transform infrared (FTIR) spectroscopy, and thermogravimetric and differential thermal analysis (TG-DTA).

Materials Characterization. Powder XRD patterns of the samples were recorded in the scan range $3 < 2\theta < 70°$ using Cu Kα_1 radiation (λ = 1.540 56 Å) on a NT 2100 Rigaku diffractometer, operating with a primary Ge monochromator. WAXS measurements were performed on a NT-2200 Rigaku diffractometer using a pinhole camera with a rotating anode generator (Ni monochromated Cu Kα_1 radiation, λ = 1.540 56 Å). For WAXS, the measurements were carried out within the scattering range $0.2133 < q < 3.45$ Å^{-1} ($0.213° < 2\theta < 50°$). WAXS patterns were first radially averaged to obtain the function $I(q)$, where $q = (4\pi/\lambda) \sin\theta$ is the scattering vector (2θ = diffraction angle; λ = 0.154 nm) and then corrected for the background scattering from the experimental setup including the use of Kapton films during the measurements.

^{29}Si and ^{13}C MAS NMR spectra were recorded with a CMX 400 NMR spectrometer (JEOL, Japan) using a 7.5 mm resonance probe. A pulse delay acquisition with a pulse delay of 120 s and a spinning frequency of 3000 Hz were employed for the measurements of the solid samples. Static measurements of ^{29}Si and ^{13}C NMR for the solutions at different reaction times were also recorded

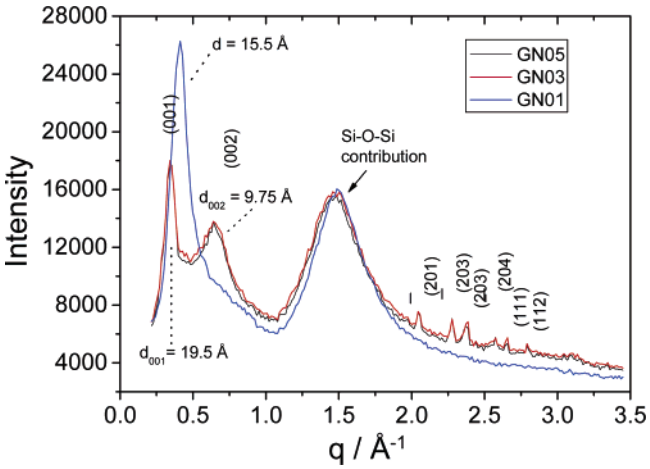

Figure 3. WAXS patterns of GN01, GN03, and GN05. The indexing of the main reflections observed and determined by powder XRD have been added for clarity.

using the CMX 400 NMR spectrometer (JEOL, Japan). Chemical shifts were estimated in ppm with respect of the reference tetramethylsilane (0 ppm).

The infrared analysis was performed by a Thermo Nicolet AVATAR 360 FTIR spectrometer in the range of 500−4000 cm^{-1} in a transmission mode and using KBr pellets. The data were collected over 32 scans with a resolution of 4 cm^{-1}.

Thermal analysis was carried out on a Thermoplus TG 8120 instrument (Rigaku Co.. Ltd., Japan) using a simultaneous TG-DTA. The samples were referenced against calcined alumina and were heated in air at a rate of 10 °C min^{-1} from 25 °C to a maximum of 600 °C.

Results and Discussion

Evolution of the Samples during Aging. The changes in the sols, immediately after the addition of GPTMS, were monitored as a function of time. The aging time was characterized by two different events: the formation of a homogeneous and transparent gel layer at the sol/air interface after 2 days for the samples GN03 and GN05 and 3 days for GN01 and the growth of ∼1−2 mm in length and ∼200−1000 μm in thickness of plate-shaped colorless crystals that occurred from the fourth reaction day in GN03 and GN05. After 10 days, full gelation occurred in all the samples, and several crystals were spread in the final transparent solids.

^{13}C NMR Characterization. The effect of NaOH on GPTMS was evaluated by ^{13}C NMR spectroscopy.[14] Figure 2 shows the reference GPTMS spectrum (liquid, spectrum a) and the ^{13}C MAS NMR solid-state spectra of the four different samples after 10 days (spectra b, c, d and e). The different carbons in GPTMS are marked from 1 to 7 (see the inset in Figure 2). Carbons in position 1, C(1), and 2, C(2), in particular, are assigned to the epoxy and can be used to monitor the effect of increasing amounts of NaOH on the ring opening (See Supporting Information for a detailed attribution of ^{13}C signals). The ring opening increases with NaOH concentration, in the order GN05 > GN03 > GN01, as indicated by the decrease in intensity of the signals C(1) and C(2) at 44 and 51 ppm, respectively (Figure 2). The

(14) The ^{13}C spectra of $CDCl_3$ in liquid state show a triplet; in spectrum a of Figure 2 only a singlet is shown because we used a solid state probe for liquid analysis, and this has produced a loss of resolution.

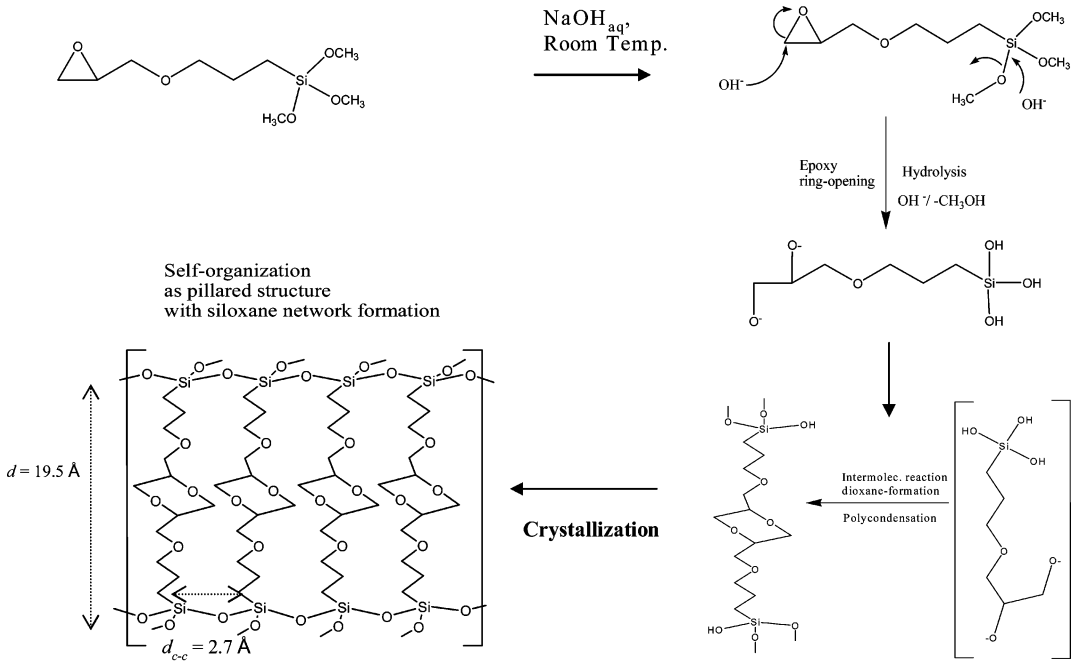

Samples	Epoxy ring-opening conversion (%)
GN01	49
GN03	77
GN05	96

Figure 4. Schematic description of the crystal formation of GPTMS in strong basic conditions: the formation of the organized bridged silsesquioxane structure with Si-substituted 2,5-bis(propoxymethyl)-1,4-dioxane as organic spacer.

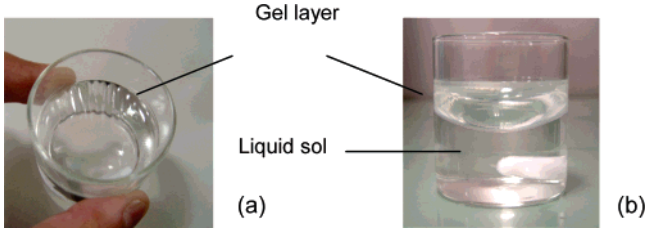

Figure 5. Pictures from the top (a) and side (b) showing the formation of a thin layer gel formed at the sol−air interface from the second reaction day and that favors the slow polycondensation of the hybrid materials and the formation of the resulting crystals.

opening of epoxy in GPTMS has, generally, the effect to form ethylene oxide chains (−O−CH_2−[CH_2−CH_2−]$_n$−O−) via polycondensation reactions of diols.[11] This reaction is accompanied by the broadening, with the increase of NaOH in the sol, of the signal at 74 ppm, which is the typical fingerprint of the formation of ethylene oxide chains in GPTMS based hybrids.[11b] However, in these particular conditions of synthesis, this is not the only possible reaction of the epoxy groups; they can also react with each other, after opening, to form a *p*-dioxane ring structure. The sharp carbon signal at 68 ppm[15] confirms the presence of dioxane groups in GN03 and GN05 (Figure 2c, 2d and 2e) but not in GN01 (Figure 2a). The ring opening has been evaluated by fitting the peak area of the ^{13}C MAS NMR signals for C(1) and C(2). In the case of GN01 the epoxy opening is low (49%) while the GN03 it results in a much higher value-(77%) and is almost completed in GN05 (96%). The decrease in intensity of the C(1) and C(2) signals is directly related to the appearance of the broad and intense peak around 74 ppm. This chemical shift value is characteristic of C atoms in oligo- or poly(ethylene oxide) derivative species formed from a ring-opening reaction of the epoxy groups.[16,17] The NMR data reveal that in high basic conditions there are two possible reaction pathways upon opening of the epoxy: formation of poly/oligo(ethylene oxide) chains or dioxane groups. The basicity of the solution is crucial to address the epoxy opening, and only when the NaOH concentration exceeds a critical value are the dioxanes formed. On the other hand the dioxanes link two GPTMS molecules giving rise to a bridged polysilsesquioxane species that favors the formation of organized structures. Figure 2e shows the ^{13}C MAS NMR spectrum of the crystal part of GN05, which was mechanically separated from the gel matrix. Because it was impossible to achieve a full mechanical isolation of the hybrid crystal, a certain amount of gel part was also measured at the same time. In the crystal rich sample, the signal at 68 ppm corresponding to a dioxane structure significantly increases in intensity, indicating that the dioxane formation is closely correlated to the crystallization. The formation of poly(ethylene oxide) was hindered within the crystal and its

(15) Kalinowski, H.-O.; Berger S.; Braun, S. *Carbon-13 NMR Spectroscopy*; Wiley and Sons: Chichester, 1988; p 349.

(16) Templin, M.; Wiesner, U.; Spiess, H. W. *Adv. Mater.* **1997**, *9*, 814.

(17) A qualitative evaluation of the length of the polyethylene oxide chains formed upon epoxy opening can be obtained looking at ^{13}C signal in the 70−74 ppm range. The formation of short oligomeric ethylene oxide chains of different length is generally revealed by the presence of overlapped sharp signals, and a broad signal is instead an indication of longer chains.

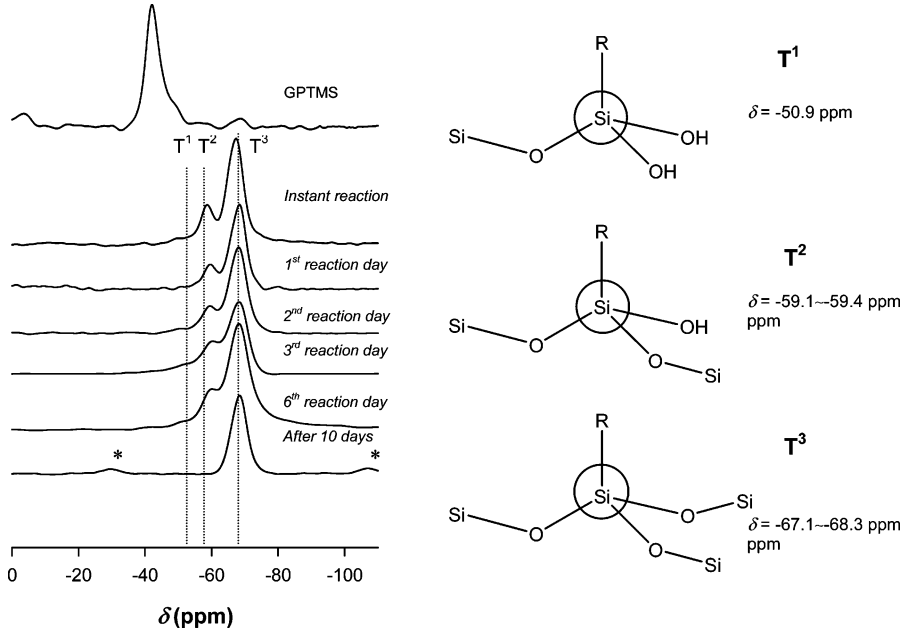

Figure 6. [29]Si solution NMR spectra for GPTMS and the sols at different aging times (the signals annotated with an asterisk correspond to the spinning bands).

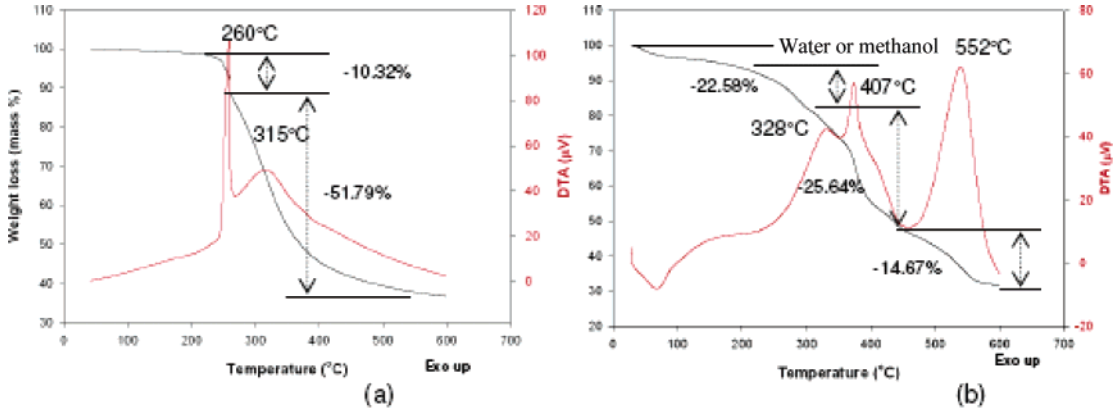

Figure 7. TG-DTA curves for the hybrid gel (sample GN01) and for the crystals embedded sample (sample GN05).

surrounding region. This was confirmed by the signal of carbon 4, C(4), being clearly observed. In addition, all the peaks in Figure 2e are very sharp, indicating that the structural variation of the crystal is rather small in comparison to the gel part (vide infra).

WAXS and XRD Analysis. The hybrid structures were studied by WAXS and powder XRD. The WAXS pattern of GN01 gel shows (Figure 3) two broad peaks: the first one, intense, at 15.5 Å ($q = 0.4$ Å^{-1}) and the second one, which is particularly broader, at 4.2 Å ($q = 1.43$ Å^{-1}). The absence of any sharp Bragg signal is an obvious sign of the absence of crystal organization, and the broad signal at 4.2 Å is due to amorphous silica. The latter peak is the Si−O−Si contribution from the silica network of the hybrid materials.[18] In some cases the presence of an additional and independent signal, such as the first intense peak at a distance of 15.5 Å, can be interpreted as a presence of short range order in the solid which is likely to be favored by the interconnected organic units after polymerization/polycondensation. The WAXS patterns of GN03 and GN05, recorded within the scattering range $0.21 < q$ (Å^{-1}) < 3.45 are, instead, very different in comparison with those of GN01. The WAXS patterns of GN03 and GN05, which appear similar, are characterized by a series of sharp and well-defined peaks. The first sharp and most intense Bragg signal is at a distance of 19.5 Å ($q = 0.32$ Å^{-1}). A set of seven additional sharp but less intense peaks are observed in the pattern. The second peak is detected at 9.75 Å ($q = 0.64$ Å^{-1}), which is at one-half distance of the first one and is attributed to its second harmonic. The patterns reveal the formation of a long-range ordered lamellar structure, which is a typical structure that could be expected to form in these synthesis conditions.[19,20] Figure 4 illustrates the proposed reaction pathway of GPTMS after ring opening for the crystal formation.

The powder XRD pattern indexed on the basis of the 00*l* lines for the crystals in sample GN05 shows that the crystals belong to a monoclinic unit cell, space group *C*2, $a = 6.30$-

(18) Boury, B.; Corriu, R. J. P. In *Supplement Si: The Chemistry of Organic Silicon Compounds*; Rappoport, Z., Apeloig, Y., Eds.; Wiley and Sons: Chichester, 2001; p 565.

(19) Moreau, J. J. E.; Vellutini, L.; Chi Man, M. W.; Bied, C.; Bantigneies, J.-L.; Dieudonnè, P.; Sauvajol, J. L. *J. Am. Chem. Soc.* **2005**, *127*, 11204−11205.

(20) Alauzun, J.; Mehdi, A.; Reyé, C.; Corriu, R. J. P. *J. Am. Chem. Soc.* **2005**, *123*, 7957−7958.

(2) Å, $b = 2.70(1)$ Å, $c = 19.51(1)$ Å, and $\beta = 92.04(2)°$.[21] (The indexing parameters for the crystals in sample GN05 are shown in Supporting Information).

The WAXS and XRD data indicate that the presence of dioxanes is directly correlated to the formation of the hybrid crystal structures. The distance of 19.51 Å, in fact, corresponds to the length of the organic spacer *R* in $O_{1.5}Si-R-SiO_{1.5}$ that should result from the reaction of two GPTMS (9.75 Å × 2) via ring opening of the epoxy. A Si-substituted 2,5-bis(propoxymethyl)-1,4-dioxane is, therefore, formed. The value of the interlayer distance fits well with the size of the organic spacer if we suppose that the organic chains are fully extended. The stacked layers along the organic pillars (Figure 4) are, in fact, at a layer-to-layer distance of 19.5 Å. The distance between two neighboring organic chains, d_{c-c}, is instead 2.70 Å, which is well in accordance with the expected center-to-center distance of two neighboring dioxane groups (2.85 Å). On the other hand this is a good indication of the role played by secondary forces between adjacent organic chains to push the self-ordering of the hybrid network. The relatively strong attraction between close chains favors the maximum packing of the hybrid network and its crystallization.

Hybrid Crystal Formation. The formation of dioxane bridged chains upon reaction of GPTMS in highly basic conditions is fast. The higher the percentage of epoxy ring opening at the first reaction stage, the easier the formation of Si-bis substituted 2,5-bis(propoxymethyl)-1,4-dioxane. This reaction is in competition with the formation of the ethylene oxide chains, and in fact, not all the gel is crystallized. It is very interesting to observe, however, that the crystals are slowly formed in the course of the gelation of the matrix. This indicates that the hybrid material has a strong tendency to self-organize. The slow solvent evaporation during gelation, together with the proceeding of the polycondensation reactions (vide infra), favor the organization because the organic chains get closer and closer and the secondary forces between close chains become more intense. It is also important to stress that the crystals, which are formed via self-organization, are in any case bounded to the hybrid network. Even if they can be considered a separate phase they are, however, covalently bonded to the hybrid material; this makes separation of the crystalline phase quite difficult, and we were not able to perform a specific analysis by electron microscopies.

After epoxy opening two different reaction pathways are possible: (1) the epoxies form poly/oligo(ethylene oxide) chains, which will give a transparent gel; (2) the epoxies form *p*-dioxanes ring structures via intermolecular reactions, and in this case crystalline hybrids can be finally observed (Figure 4). The homopolymerization of non-silica-based DGEBA (di-glycidyl ether of bisphenol A)/TETA (triethylene tetramine) epoxy systems has been reported in the literature leading to the formation of *p*-dioxane ring structures as the minor compound at room temperature using sterically hindered tertiary amines as weak base catalysts.[22] The use of a strong base seems to promote the formation of dioxane ring structures also in organosilica epoxy systems. As shown in Figure 2, the sharp and intense signal of dioxane in the ^{13}C NMR spectrum for the crystal particle enriched part (Figure 2e), in comparison with that for whole material (Figure 2d), was observed at 68 ppm, following the previous consideration that the *p*-dioxane is closely related to the crystal formation. In addition, the formation of poly(ethylene oxide) chains was hindered around the crystal part. It should also be noticed that more intense signals corresponding to epoxy groups (44 and 51 ppm) are observed for the crystal rich gel with respect to the gel matrix. This may be explained if we suppose that the interface between the crystal and the amorphous part is mainly formed by unreacted epoxy groups.

The evolution of the sol during aging is thus of primary importance. The basic conditions that are employed play an important role on the evolution of the sol and on the texture of the final hybrid materials. During sol aging at room temperature, a transparent gel film developed and covered the sol (Figure 5). This layer contributes to the slow evaporation and slow polycondensation reaction rate. These conditions favor self-organization within the hybrid. It is worth noting that this slow polycondensation is also due to the low temperature of processing; the experiments were carried out at 20 °C.

Before the sol−gel transition, the polycondensation process is then kinetically controlled, and while the Si−O−Si bonds are progressively formed, the organic units are brought to each other favoring interactions via secondary forces and their auto-organization. The ^{29}Si NMR spectra of the sol GN05 show that the silica reactions are completed after 10 days (Figure 6). The final product is similar for the three different samples, and the presence of only $SiC(OSi)_3$ (T^3) species indicates a high degree of final condensation. They show, however, a different polycondensation rate during gelation. A comparison of the spectra at different gelation times reveals, in fact, that in GN03 and GN05 polycondensation is faster than in GN01. T^1 species are observed up to two reaction days in GN01 but not in GN03 and GN05 (Figure 6).

The partial polycondensation of the inorganic side has also the advantage to make the hybrid structure flexible, at least until crystallization. A "softer" matrix can also contribute to an ordered structure formation. On the other hand the weak interactions between precursor molecules during the hydrolysis and condensation of $(RO)_3Si-R'-Si(OR)_3$ have been also shown to influence the kinetic parameters of the gelation and to modify the texture of the resulting amorphous bridged silsesquioxanes.[7]

At the end of the process, full polycondensation of the silica (Si−O−Si) is demonstrated by ^{29}Si MAS NMR (Figure 6). The final gel (10 days of aging) shows only one intense signal at −68 ppm due to T^3 species. This finding is in agreement with the ^{13}C MAS NMR (Figure 3) and confirms the high degree of polycondensation of the final materials.

(21) Indexing of the powder X-Ray reflections has been carried out using the CRYSFIRE powder indexing program and refined using Cell refinement program. Shirley, R. *CRYSFIRE system for automatic powder indexing*; The lattice Press: Guildford, U.K., 2000.

(22) D'Almeida, J. R. M.; Menezes, G. W. D.; Monteiro, S. N. *Mater. Res.* **2003**, *6*, 415.

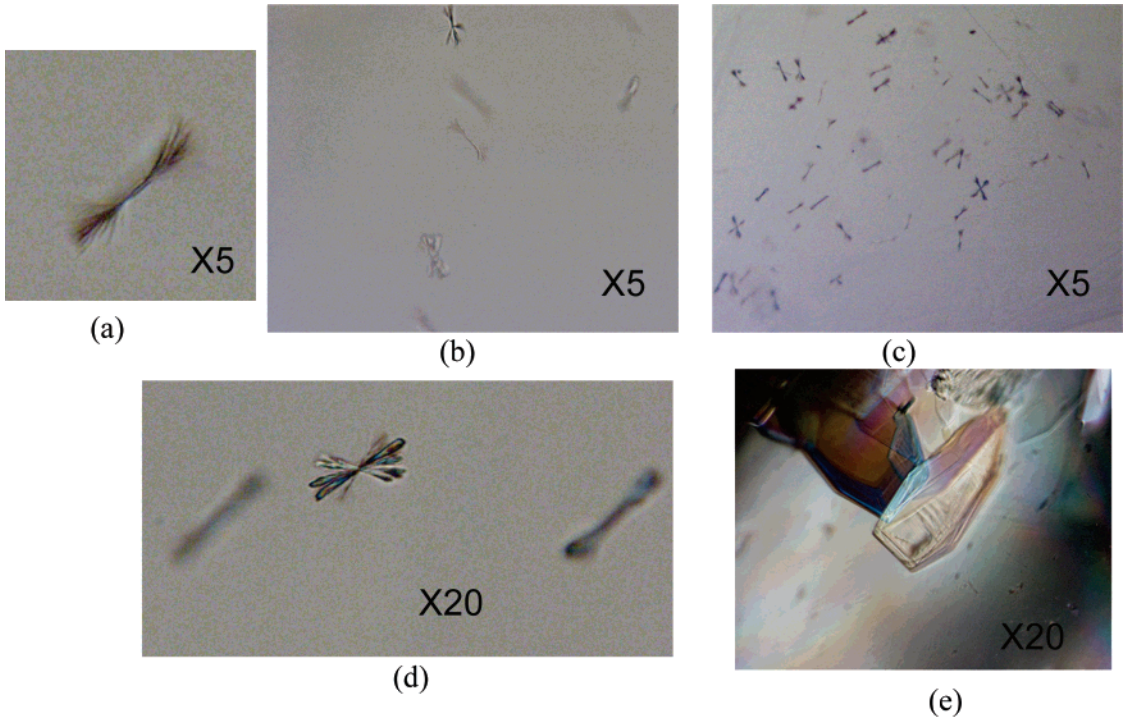

Figure 8. Pictures from a polarized optical microscope showing the crystal evolution: (a) aggregation; (b, c, d) nucleation; (e) crystals in the growing oligomer.

The broadening and the shift of the GPTMS carbon signal C(6) (CH_2 group in α-position of the silicon) from 4.5 ppm (GPTMS) to 9 ppm (resulting products) indicate, in fact, a more restricted environment and lower mobility of the species.

The infrared spectra (not shown in the figures) of the three samples GN01, GN03, and GN05 show an intense Si−O−Si absorption band at 1050 cm^{-1} and no signals related to residual silanol groups (Si-*OH*) at 3300−3500 cm^{-1}. The spectra are in agreement with a high level of final polycondensation.

TG-DTA curves confirm that the intimate structure, after gelation, is highly polycondensed. The absence of a significant weight loss before 200 °C suggests, in fact, that no polycondensation occurs any more from residual silanols. For the gel sample (GN01) which does not exhibit any crystals formation, the TG-DTA curves (Figure 7a) show two observable step weight losses between 250 °C and 500 °C due to the decomposition of the organic groups of poly (oligo) cross-linked organic chains (with poly(ethylene oxide) chains and remaining epoxy groups). These weight losses are characterized by two exothermic signals at 260 °C and 315 °C. The TGA curves indicate an overall weight loss of 62%. In the crystals embedded sample (sample GN05), the weight loss observed in the first part of the TGA curve (Figure 7b) and starting below 100 °C is considered to be mainly due to the evaporation of residual water or methanol, because the endothermic signal in the DTA curve is rather weak. The overall weight loss is comparable to GN01 (62.89%), but it was interesting to note a further weight loss step between 500 °C and 700 °C compared to the sample GN01, with a strong exothermic DTA signal at 552 °C. We have attributed the further weight loss of 15% to the presence of the crystals with the pyrolysis of the Si-substituted 2,5-bis(propoxymethyl)-1,4-dioxane organic spacer which may show higher thermal stability compared to the poly(ethylene oxide) chain in a step-like structure. The percentage of crystallization in the sample GN05 is then evaluated to 23%.

We have followed the crystal growth in the gel phase by taking several polarized optical microscope pictures of GN05 at different aging times (Figure 8). During aging, the hybrids in solution aggregate, then nucleate, and finally grow into crystals. The formation of the gel layer at the sol/air interface is an additional factor facilitating the slow growth of the crystals (vide supra). This layer reduces the rate of water evaporation, which in turn adjusts the crystal growth rate so that it provides fewer, larger crystals. In addition, we can observe the different stages of the crystallization process such as the aggregation step which occurs generally too fast in other materials.[23] In Figure 8 we can observe a cloud of small interconnected crystals resulting from the nucleation that becomes larger with time. The oriented aggregations of the interconnected crystals will then determine the shape of the crystals (polygonal thin-plate shaped crystals).

Conclusions

Hybrid organic−inorganic materials have been synthesized by a solvent-free reaction of GPTMS in strong basic conditions, using NaOH as the catalyst. The NaOH concentration is very important to control the epoxy opening reactions; higher amounts of NaOH produce a more efficient opening. Two possible reaction pathways are observed after epoxy opening: (1) formation of poly/oligo(ethylene oxide) chains interconnected to the silica network which will give

(23) Heywood, B. R.; Mann, S. *Adv. Mater.* **1994**, *6*, 9.

a transparent gel and (2) formation of *p*-dioxanes ring structures via intermolecular reactions; in this case crystalline hybrids are finally observed.

The formation of a gel layer at the sol−air interface favors the self-organization of the hybrid because it reduces the evaporation rates and the kinetics of polycondensation. These conditions give the formation of crystalline aggregates with a layered structure, as shown by WAXS and SAXS characterization.

The experiment has shown that self-ordered long-range organization in hybrid materials can be achieved in much more general conditions than previously thought.

Acknowledgment. The authors are grateful to Prof. T. Kanaya and Dr. T. Konishi for WAXS measurements. This work is also partly supported by the Grants-in-Aid from the Ministry of Education, Science, Sports and Culture, Japan, Nos. 16686041 and 13305061. PRIN Italian Projects (2005039071_005) are also acknowledged for financial support.

Supporting Information Available: Main chemical shifts from the ^{13}C MAS NMR spectra and XRD parameters calculated for GN05 (PDF). This material is available free of charge via the Internet at http://pubs.acs.org.

CM062660U